

Finite Element Analysis of Axial Compression Performance of High-Strength Recycled Concrete Composite Columns with Built-In Square Steel Tube

Hao Liang¹, Yanling Guo^{2,*}

¹Hao Liang, Undergraduate students, Southwest Jiaotong University, Chengdu, 610031, P.R. China

²Yanling Guo, Undergraduate students, Southwest Jiaotong University, Chengdu, 610031, P.R. C

*Corresponding author: 18881902233@163.com

Received February 09, 2024; Revised March 10, 2024; Accepted March 17, 2024

Abstract To study the axial compression performance of high-strength recycled concrete columns with built-in square steel tubes, ABAQUS software was used to model and analyze two existing test specimens, verifying the accuracy of the model. On the basis of a reliable model, parameter analysis was conducted on 13 specimens, with variable parameters including square steel tube thickness, square steel tube strength, and slenderness ratio. The results showed that the established finite element model exhibited longitudinal reinforcement buckling and steel tube tearing deformation consistent with the experimental results, and the height of the load axial displacement curve was consistent. The average error of the ultimate bearing capacity was within 5%; The increase in steel tube thickness has little effect on the axial compression bearing capacity and stiffness, while the increase in steel tube yield strength has a significant impact on the axial compression bearing capacity and residual bearing capacity; With the increase of slenderness ratio, the axial compression stiffness and ultimate bearing capacity of composite columns are obviously degraded. A numerical calculation method between the axial compression stability coefficient and slenderness ratio is fitted, which can be used as a reference for the design of composite columns.

Keywords: Built-in square steel tube, High strength recycled concrete, Stacked column, Axial compression performance, finite element analysis

Cite This Article: Hao Liang, and Yanling Guo, "Finite Element Analysis of Axial Compression Performance of High-Strength Recycled Concrete Composite Columns with Built-In Square Steel Tube", *American Journal of Civil Engineering and Architecture*, vol. 12, no. 2 (2024): 30-35. doi:10.12691/ajcea-12-2-2.

1. Introduction

Recycled aggregate concrete (RAC) is a type of concrete that reconstructs waste concrete by crushing and sieving it, then adding cement, water, and fine aggregates. Many studies have shown that as long as it is properly blended, the mechanical properties of RAC are comparable to those of natural aggregate concrete (NAC) [1,2]. Therefore, many scholars have applied it instead of ordinary concrete in traditional structures. However, some studies have shown that the deformation of RAC is greater than that of NAC, so it is necessary to apply constraints in the structure to ensure the safety of RAC structure [3]. This includes the installation of steel tubes inside the RAC, which not only fully utilizes the advantages of steel tube RAC columns, but also overcomes the disadvantages of corrosion resistance, poor fire resistance, and complex beam column node treatment of steel tube RAC columns, making RAC widely used in the field of building structures.

Many scholars have conducted in-depth research on the mechanical properties of composite columns with NAC embedded steel tubes, including experimental, finite

element, and theoretical studies [4,5,6,7]. The results indicate that the concrete, steel tubes, and longitudinal steel bars in the composite column can play a good synergistic and complementary role. However, there is relatively little research on the mechanical properties of laminated columns with RAC embedded steel tubes both domestically and internationally. He et al. [8,9] conducted axial compression and eccentric compression tests on RAC reinforced concrete columns with built-in circular steel tubes. The results showed that the eccentric compression failure process and bearing performance of steel tube RAC composite columns were similar to those of ordinary concrete. Due to the presence of internal steel tubes, RAC was well constrained.

With the increasing structural requirements of modern architecture, ordinary strength concrete is no longer sufficient to meet the requirements, and high-strength concrete is often required in super high-rise structures. Niu et al. [10,11] conducted axial compression tests on high-strength RAC columns with built-in circular and square steel tubes, and the results showed that the bearing capacity of square steel tube high-strength RAC composite columns was improved compared to NAC composite columns. However, there is relatively little

research on this type of composite column, and the influence of different factors on its axial compressive bearing capacity is not yet clear. Therefore, in order to investigate the influence of different factors on the axial compression performance of high-strength RAC columns with built-in steel tubes, this paper conducts modeling and simulation analysis on two specimens in existing research. After verifying the accuracy of the model, the influence of steel tube thickness, steel tube strength, and aspect ratio on axial compressive bearing capacity was explored, aiming to provide reference for engineering.

2. Overview of Existing Experiments

Two specimens from Reference [11] were selected for simulation verification, which were designed with steel tube thickness as a variable. The cross-sectional design is shown in Figure 1. The detailed design parameters of the test specimens and parameter analysis specimens are shown in Table 1. The cross-sectional dimensions of the specimens are all 230mm × 230mm, with a height of $H=1150$ mm. The reinforcement is composed of four longitudinal bars with a diameter of 12mm, and the diameter of the hoop bars is 6mm. The spacing between the test sections is 100mm, and the inner steel tube is a square steel tube with a side length of 100mm. The longitudinal reinforcement and hoop reinforcement use HRB400 grade ordinary steel bars with yield strengths f_y of 415MPa and 495MPa respectively, and the yield strength f_y of steel tubes is 378MPa. The high-strength RAC cube has a compressive strength of 62.7 MPa and an elastic modulus of 37400 MPa.

The axial compression test was conducted on an electro-hydraulic servo press with a ultimate load of 5000kN. After a preload of 400kN, the load was unloaded and officially started. The experiment adopts a load

control loading system, with each level holding the load for 5 minutes. The test is stopped when the load decreases to 65% of the peak load. The test results indicate that all specimens exhibit failure modes such as concrete cover peeling, longitudinal reinforcement buckling, hoop bulging, and steel tube bulging.

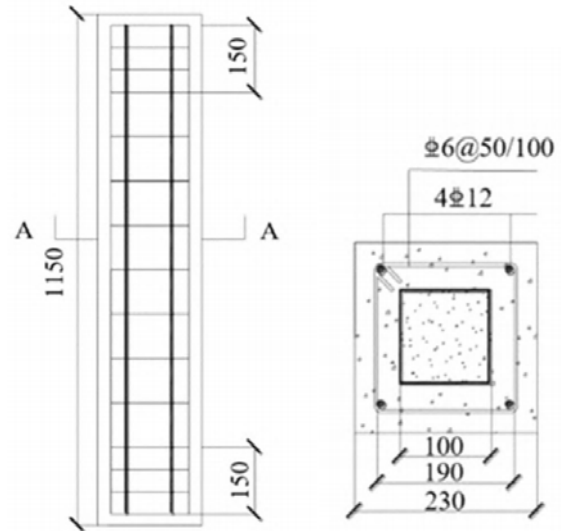


Figure 1. Structural diagram of specimen

Table 1. Specimen Design Parameters

Specimen. No	t/mm	f_{ys}/MPa	H/mm	λ	P_p/kN
RCFSSST	4	378	1150	17.3	2986.0
RCFSSST-3	4.5	378	1150	17.3	3583.2

where: λ is the slenderness ratio of the specimen, calculated as $\lambda=H/\sqrt{(I/A)}$; I is the radius of rotation; A is the cross-sectional area.

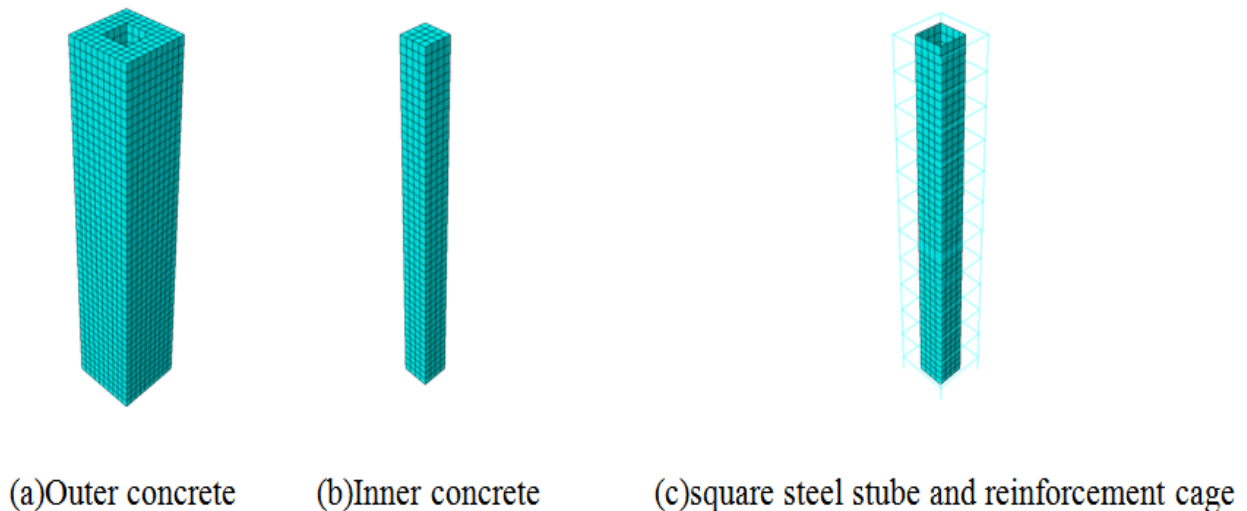


Figure 2. Model components and grid division

3. Finite Element Model

3.1. Geometric Models and Mesh Partitioning

In order to simulate the mechanical evolution of laminated columns more realistically, a separate modeling method was adopted to independently model the inner and outer concrete of the steel tube, and rigid pads were arranged on both sides to ensure convergence. At the same time, to ensure computational efficiency and accuracy, the global grid size was determined to be 25mm after multiple trials, and all components are shown in Figure 2.

3.2. Material Properties and Mesh Types

(1). High strength RAC

The solid mesh (C3D8R) was adopted as the unit for high-strength RAC. For the constitutive relationship of high-strength RAC, based on the material test results of Tian et al. [12] using high-strength RAC, combined with Guo et al. [13], the constitutive relationship of concrete was proposed, and the uniaxial compressive stress-strain relationship curve of high-strength RAC was proposed:

$$y = \begin{cases} 2.46x - 1.92x^2 + 0.46x^3 & 0 \leq x \leq 1 \\ \frac{x}{8.63(x-1)^2 + x} & x \geq 1 \end{cases} \quad (1)$$

$$y = \frac{\sigma}{f_c}, \quad x = \frac{\varepsilon}{\varepsilon_c} \quad (2)$$

where: f_c and ε_c represent the ultimate compressive stress and ultimate compressive strain of concrete, respectively.

(2). Steel

The constitutive relationship between steel tubes and steel bars adopts a simplified double line ideal plastic model [14] (as shown in Figure 3), which is the elastic section before yield, the plastic strengthening section from yield to ultimate strength, and the slope of the strengthening section is 0.01 times that of the elastic section. The use of truss elements (T3D2) for steel reinforcement units and shell elements (S4R) for steel tube units can better converge the calculation while ensuring the calculation results.

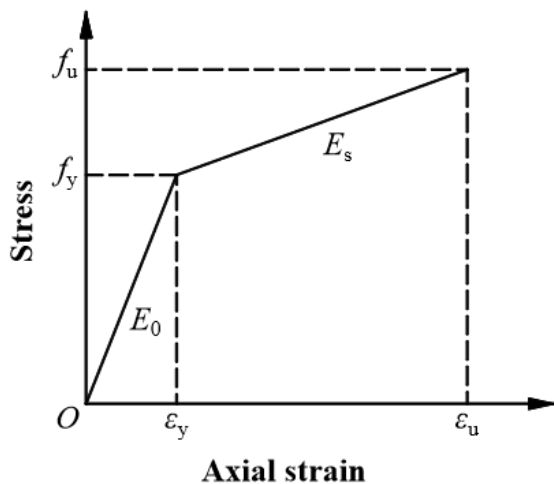


Figure 3. Schematic diagram of reinforcement constitutive relationship

3.3. Interaction

To avoid stress concentration, rigid pads were installed on the upper and lower surfaces of the specimens, which were connected to the upper and lower surfaces of concrete and steel tubes through binding constraints. The steel cage is combined with the outer concrete by embedding, ignoring the relative sliding between the steel and concrete. In order to restore the constraint effect, face-to-face contact is adopted between the outer wall of the concrete steel tube and the inner wall of the concrete steel tube, taking into account the contact separation between the steel tube and the concrete. The contact properties are set to: hard contact in the normal direction, penalty function in the tangential direction, and friction coefficient of 0.5 [15,16].

3.4. Boundary Conditions and Loading Methods

Based on the experimental results, the displacement and rotation around the longitudinal axis in the lower three directions of the specimen were constrained, and the lower hinge was simulated, with an axial displacement of 20mm applied to the upper part.

3.5. Model Validation

The comparison of load axial displacement curves of two high-strength RAC column specimens with built-in square steel pipes simulated is shown in Figure 4. Overall, the average error of the simulated ultimate bearing capacity is 3.7%. The trend of the curve is basically consistent, and it rapidly decreases after reaching the peak point, entering a gentle downward section due to the plasticity of steel bars and steel tubes. The curve stiffness of finite element simulation is relatively high. This model has been debugged through mesh, constitutive, and boundary analysis, and it has been found that the effect is not significant. However, the curve trend is in good agreement with the experiment. According to the results of existing literature, this is highly likely an error in the experiment. During the loading process of concrete, the compaction process of internal voids will produce virtual displacement, so the axial compression stiffness of the test results is smaller. But it does not affect the subsequent bearing capacity analysis, as the error in bearing capacity is relatively small.

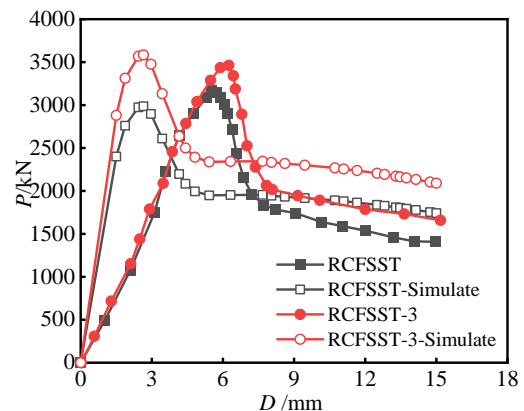


Figure 4. Comparison of finite element results

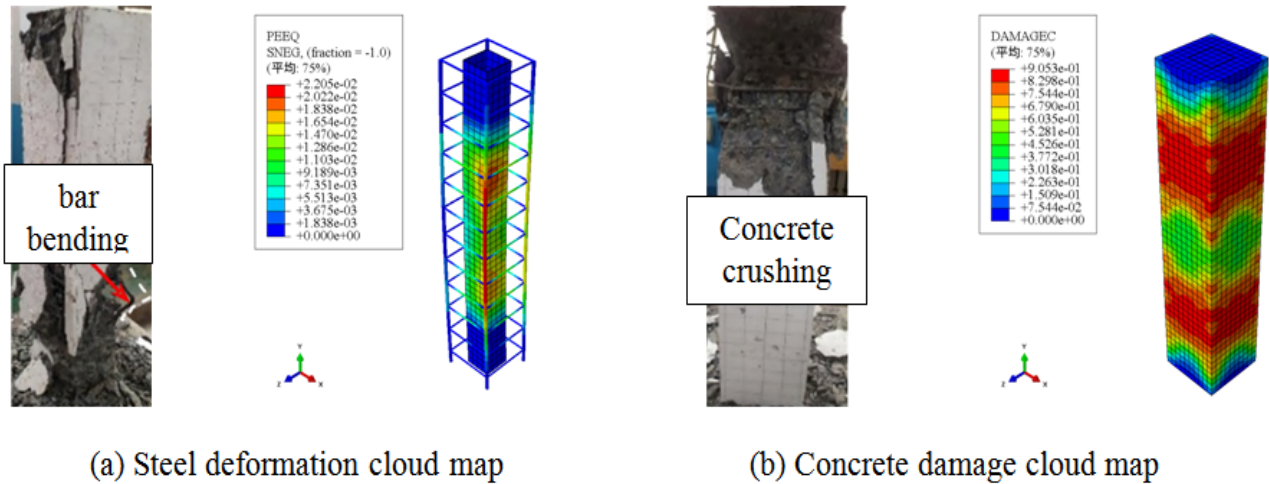


Figure 5. Comparison of failure modes

Figure 5 shows a comparison of experimental and finite element failure modes. The experimental results show that when reaching the ultimate state, one side of the longitudinal reinforcement bends and the steel tube corners tear. As shown in Figure 5a, the finite element method effectively reproduces this phenomenon. There is a significant plastic deformation (PEEQ) in one side of the reinforcement and the steel tube corners, indicating a high stress at this point. Figure 5b shows the failure mode of concrete, and the compressive damage mode of concrete given by the finite element method is the appearance of X-shaped concrete crushing at the upper and lower ends. The experimental results show that one end of the concrete has a large area of crushing and peeling, which is in good agreement. The established finite element model has been validated and can be further analyzed for parameters.

Table 2 Extended specimen design parameters

Specimen. No	t/mm	f_{ys}/MPa	H/mm	λ	P_p/kN	Note
FE-1	2	378	1150	17.3	2927.1	Changes in steel tube thickness
FE-2	3	378	1150	17.3	2957.0	
FE-3	4	378	1150	17.3	2986.0	
FE-4	5	378	1150	17.3	3014.0	
FE-5	6	378	1150	17.3	3041.3	
FE-6	4	235	1150	17.3	2606.0	Changes in yield strength of steel tubes
FE-7	4	335	1150	17.3	2744.3	
FE-8	4	400	1150	17.3	3356.0	
FE-9	4	450	1150	17.3	3604.8	
FE-10	4	378	1500	22.6	2925.6	Change in aspect ratio
FE-11	4	378	2500	37.6	2812.5	
FE-12	4	378	3000	45.1	2772.3	
FE-13	4	378	3500	52.7	2771.0	

4. Parameter Analysis

According to Section 3.5 of this article, it can be seen that the finite element model established in this article can accurately describe the axial compressive mechanical behavior of high-strength RAC columns with built-in square steel tubes. Therefore, the RCFSSST model, which has a high degree of agreement between the load axial displacement curve and the failure mode, was selected as

the benchmark. Thirteen models were designed with steel tube thickness, yield strength of steel tubes, and slenderness ratio as variable parameters for calculation. The specific parameters and calculation results are shown in Table 2.

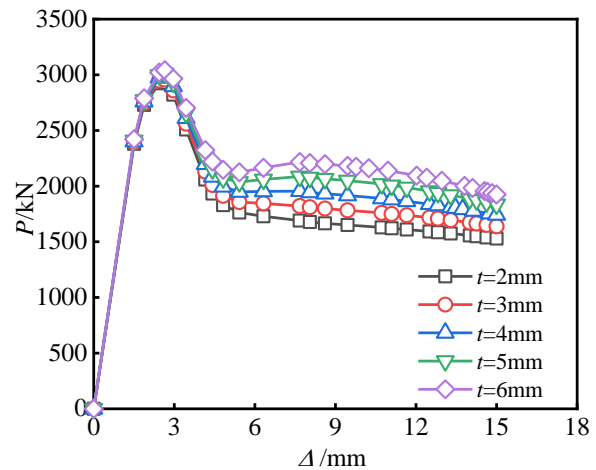


Figure 6. The influence of steel tube thickness on the load axial displacement curve

4.1. Steel tube Thickness

Figure 6 shows the effect of different steel tube thicknesses on the load axial displacement curve of high-strength RAC columns with built-in square steel tubes. As shown in the figure, the thickness of the steel tube has little effect on the elastic section of the curve. As the thickness of the steel tube increases, the residual load increases, indicating that increasing the thickness of the steel tube can effectively improve the residual deformation capacity and energy dissipation capacity of the laminated column. Compared to specimens with a steel tube thickness of 2mm, the ultimate bearing capacity of specimens with a steel tube thickness of 3mm, 4mm, 5mm, and 6mm increased by 1.0%, 2.0%, 2.9%, and 3.9%, respectively. Overall, the increase in steel tube thickness resulted in an increase of less than 5% in axial compression bearing capacity, indicating a lower efficiency in improvement. The reason for this may be that although the increase in steel content increases the

confinement coefficient of steel tubes on the concrete in the core area, the increase in confinement is relatively small due to the small area of concrete in the core confinement area, which accounts for a lower proportion of the entire cross-section.

4.2. Yield Strength of Steel Tubes

Figure 7 shows the effect of steel tube yield strength on the load axial displacement curve of high-strength RAC columns with built-in square steel tubes. As shown in the figure, the ultimate bearing capacity and residual load of the composite column show a significant increase with the increase of the yield strength of the steel tube, but the axial compression stiffness does not change much. Compared with the specimens with a yield strength of 235MPa, the ultimate bearing capacity of specimens with a yield strength of 335MPa, 378MPa, 400MPa, and 450MPa increased by 5.6%, 14.5%, 28.7%, and 38.3%, respectively. Improving the yield strength of square steel tubes can effectively enhance the bearing capacity and deformation capacity of laminated columns.

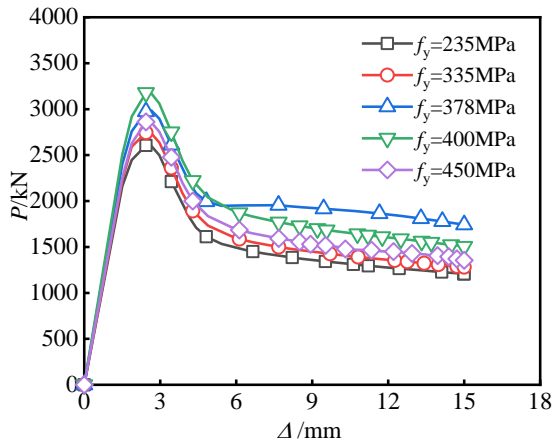


Figure 7. Effect of yield strength of steel tubes on load axial displacement curve

4.3. Slenderness Ratio

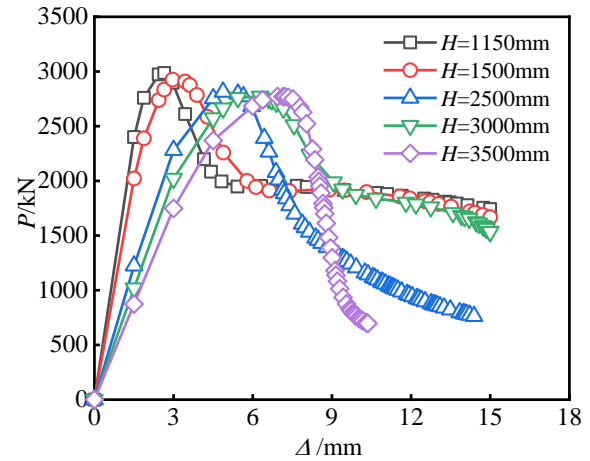
Figure 8 shows the influence of different aspect ratios on the load axial displacement curve and failure mode of high-strength RAC columns with built-in square steel tubes. As shown in Figure 8a, with the increase of slenderness ratio, the axial compressive stiffness and ultimate bearing capacity of the laminated column gradually decrease. This is because the increase of slenderness ratio leads to a significant second-order effect stress of the specimen, causing overall instability of the specimen (Figure 8b), resulting in degradation of the bearing capacity and axial compressive stiffness. Compared to the specimen with a height of 1150mm, the ultimate bearing capacity of specimens with heights of 1500mm, 2500mm, 3000mm, and 3500mm decreased by 2.1%, 5.8%, 7.2%, and 7.3%, respectively.

In the design specifications for concrete structures, the stability coefficient φ is a key parameter for calculating the axial compressive bearing capacity, which is directly related to the slenderness ratio. In previous experiments, only short column tests were conducted on this type of

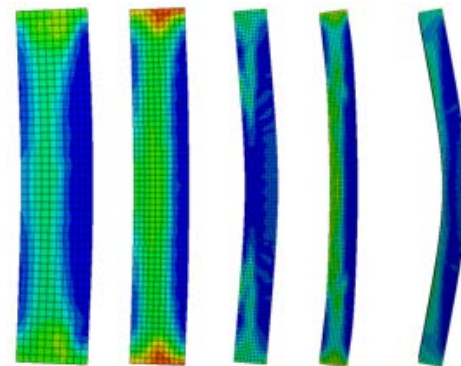
composite column, and the calculation method of bearing capacity has not yet considered the influence of stability coefficient φ . Therefore, based on the finite element analysis results, the numerical relationship between the stability coefficient φ and the slenderness ratio λ was fitted, as shown in Figure 9. The calculation method is:

$$\varphi = 5.8 \times 10^{-5} \lambda^2 - 0.00615 \lambda + 1.088 \quad (3)$$

The correlation coefficient R^2 of the fitting result is 0.996, which has a high degree of agreement and can provide assistance for the design of this type of stacked column.



(a) The influence of aspect ratio on the load axial displacement curve



(b) The influence of aspect ratio on the failure mode

Figure 8. Influence of Slenderness Ratio

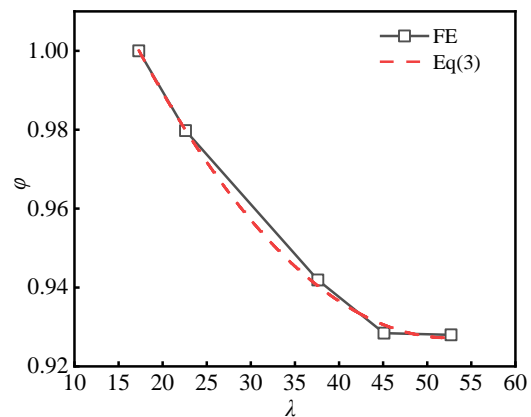


Figure 9. Influence of aspect ratio on ultimate bearing capacity

5. Conclusion

By conducting finite element modeling analysis on the axial compression performance of 13 high-strength RAC columns with built-in square steel tubes, the following conclusions were obtained:

(1) The ABAQUS finite element analysis software was used to simulate and analyze the axial compression test of high-strength RAC columns with built-in square steel tubes. The load axial displacement curve and failure mode calculated by the finite element method were in good agreement with the experimental results.

(2) The increase in thickness of steel tubes has little effect on the axial stiffness and bearing capacity of laminated columns. The increase in yield strength of steel tubes can increase the axial bearing capacity by nearly 40% within the experimental range. Increasing the thickness and yield strength of steel tubes can both enhance residual loads.

(3) As the slenderness ratio increases, the axial stiffness and axial bearing capacity of the laminated column show significant degradation, with a maximum degradation of 7.3% in the experimental range. Based on the results of finite element analysis, the axial compression stability coefficient and slenderness ratio were fitted.

Author Contribution Statement

1 Mr. Hao Liang: Conceptualization, Formal analysis, Software, Writing-original draft.

2 Mr. Yanling Guo: Conceptualization, Writing-review & editing

Conflicts of Interest

The authors claim no conflicts of interest.

References

- [1] Xiao Jianzhuang, Zhang Hanghua, Tang Yuxiang, et al. Principles of Recycled Waste Concrete and Basic Issues of Recycled Concrete. Science Bulletin, 2023,68 (05): 510-523.
- [2] Chen Zongping, Xu Ruitian, Liang Houran. Stress strain constitutive relationship and finite element analysis of recycled pebble concrete after high-temperature water spray cooling. Materials Review, 2021,35 (13): 13032-13040.
- [3] MEDNA C, ZHU W Z, HOWNF T, et al. Influence of mixed recycled aggregate on the physical mechanical properties of recycled concrete. Journal of Cleaner Production, 2014 (68) 216-225.
- [4] Yang Jian, Guo Xiaogang, Lv Xian. Experimental study on the bearing capacity of elliptical steel tube concrete. Journal of Hunan University of Arts and Sciences (Natural Science Edition), 2012,24 (01): 63-65.
- [5] Kang Hongzhen, Qian Jiaru. Experimental study on the axial compressive bearing capacity of steel tube high-strength concrete composite columns. Building Structure, 2011, 41 (06): 64-67.
- [6] Kang Hongzhen, Qian Jiaru. Test and analysis of axial compressive bearing capacity of steel tube high-strength concrete composite columns. Journal of Building Structures, 2010,31 (S1): 360-364.
- [7] Liao Feiyu, Han Linhai. Study on the mechanical properties of square steel tube concrete composite columns. Engineering Mechanics, 2010,27 (04): 153-162.
- [8] Ke Xiaojun, Yang Chunhui, Su Yisheng, et al. Experimental study on eccentric compression performance of steel tube recycled concrete composite columns. Journal of Applied Fundamentals and Engineering Science, 2020,28 (02): 354-365.
- [9] Ke Xiaojun, An Jin, Liao Dingguo, et al. Analysis of axial compression performance of fully recycled concrete composite columns with built-in steel tubes. Journal of Building Structures, 2017, 38 (S1): 291-296.
- [10] Niu Haicheng, Gao Jinlong, Zhang Yaorong, et al. Experimental study on the axial compression performance of high-strength recycled concrete composite columns with square steel tubes. Experimental Mechanics, 2022, 37 (06): 921-932.
- [11] Niu Haicheng, Gao Jinlong, Ji Jiakun et al. Axial compressive performance of high-strength recycled concrete composite columns with steel tubes. Journal of Composite Materials, 2022, 39 (08): 3994-4004.
- [12] Tian Liangliang Research on the mechanical properties of high-strength recycled concrete columns with round steel tubes. North China University of Technology, 2018.
- [13] Guo Zhenhai. Principle analysis of reinforced concrete. Beijing: Tsinghua University Press, 2003.
- [14] Liu Qin, Ma Shicheng, Yin Changjun. Implementation of elastic modulus of steel fiber reinforced concrete in finite element numerical simulation. Journal of Hunan University of Arts and Sciences (Natural Science Edition), 2014,26 (04): 35-38.
- [15] Han Linhai, Tao Zhong, Wang Wenda. Modern Composite and Hybrid Structures: Experiments, Theory, and Methods. Beijing: Science Press, 2009.
- [16] Zheng Liang, Jin Xiaojun, Dong Yanli. Compressive performance of reinforced square steel tube concrete columns. Journal of Jiangsu University (Natural Science Edition), 2015,36 (04): 469-474.



© The Author(s) 2024. This article is an open access article distributed under the terms and conditions of the Creative Commons Attribution (CC BY) license (<http://creativecommons.org/licenses/by/4.0/>).